Jordan Journal of Mathematics and Statistics (JJMS) 12(3), 2019, pp 431 - 453

PERISTALTIC TRANSPORT OF EYRING-POWELL NANOFLUID IN A NON-UNIFORM CHANNEL

ASHA. S. K [1] AND SUNITHA G. [2]

Abstract. In this paper, the effect of MHD peristaltic Transport of Eyring-Powell Nanofluid in a non-uniform channel is studied under long wavelength and low Reynolds number assumptions. Thus peristalsis of Eyring-Powell nanofluid followed through the conservation principles of mass, momentum, energy and concentration has been modelled. The peristaltic transport equations involves the combined effects of Brownian motion and thermophoresis diffussion of nanoparticles. Expressions for the velocity, temperature and concentration are obtained. The effect of various physical parameters on the flow characteristics are shown and discussed with the help of graphs.

1. Introduction

The peristalsis is derived from Latin word and comes from the Greek *peristallein*. The mechanism of peristalsis is used for pumping physiological, industrial and other forms of fluids from one place to another. Peristalsis is a mechanism of fluid transport when a progressive wave of area contraction or expansion propagates along its length. This phenomenon widely occurs in several physiological, industrial and biomedical applications such as swallowing of food through esophagus, the movement of chyme in entire gastro intestinal tract, the transport of spermatozoa in the cervical canal,

2000 *Mathematics Subject Classification.* 76A05, 76D05, 76E25, 76Z05.

Key words and phrases. Peristaltic transport, MHD, Eyring-Powell nanofluid, non-uniform channel.

Received: Jun. 28, 2018 Accepted: Nov. 11, 2018 .

transport of bile in bile duct, transport of cilia and is widely applicable in industries where direct contact with boundaries are prohibited. Some examples include finger, hose and roller pumps, food and beverage industry, cell separation, mining, pharmaceutical industry also some bio-mechanical instruments are heart-lung machine, blood pump machine and dialysis machine. Latham [1] was the first initiated the concept of peristaltic mechanism in 1966, a number of analytic, numerical and experimental studies of peristaltic flow of different fluids have been reported under different conditions with reference to physiological and mechanical situations. After the work of Latham [1], Jaffrin and Shapiro [2] investigated the peristaltic pumping. They made the study under the assumption of long wavelength and low Reynolds number approximation. Influence of magnetic field on peristaltic flow has gained much attention nowadays, due to its numerous applications in biomedical and engineering. MHD principles are useful in the design of heat exchangers, pumps, radar systems, power generation development of magnetic devices, cancer tumor treatment, hypothermia and blood reduction during surgeries. It is realized that the principles of magneto hydrodynamics find extensive applications in bioengineering and medical sciences. Mekheimer [3] studied the peristaltic blood flow under the effect of magnetic field in non-uniform channel, considering couple stress fluid as a blood model. Asha et al. [4-7] studied the effect of magnetic field and an endoscope on peristaltic motion. One of the paper, they investigated the peristaltic transport of magnetic fluid through porous media in a uniform and non-uniform annulus. Hence several researchers having such important in mind extensively discussed about the peristalsis with magnetic effect [8-14].

Nanofluid is a fluid containing nanometer sized particles called nano particles. The nano particles used in nonofluids are typically made of metals, oxides, carbides or carbon nanotubes, nanofibers, droplet, nanosheet etc. peristalsis in connection with nanofluids has application in biomedicines, i.e., cancer treatment, radio therapy etc.

Chio [15] was the first to introduce the word nanofluid that represents the fluid in which nanoscale particles (diameter less than 50nm) are suspended in the base fluid.

Nanofluid has become now the major attention of various researchers for the new manufacturing of automotive and plant cooling systems and for transfer of heat in different heat exchanger devices. Modern drug delivery systems make use of the magnetic-nanoparticles to enhance the specificity and efficiency of the drug action. Magnetic fluxes are used in the magnetic drug system for the delivery of magnetic nanoparticles loaded with drug to the tumor site. It is possible to systematically control and guide the magneto-nanoparticles towards the tumor site within the human body by means of an externally applied magnetic field. Although the idea of controlled drug delivery came to light few decades back yet the field of magnetic drug delivery has received much attention. Recently a detailed examination of nanofluid was discussed by Akbar et al. [16] with slip effects on the peristaltic transport of nanofluid in an asymmetric channel. They extended their paper by considering endoscope effects on the peristaltic transport of nanofluids in non-uniform channel [17]. A numerical study for MHD peristaltic flow considering Williamson nanofluid model in an endoscope with partial slip and wall properties was studied by Hayat et al. [18]. Nanofluid exhibiting advance thermal properties, having higher thermal conductivity and heat transfer coefficient as compared to the base fluid. Mixed convection MHD peristaltic flow of Jeffery nanofluid with Newtonian heating was investigated by Akbar et al. [19]. A numerical study of peristaltic flow of MHD Jeffery nanofluid in curved channel with convective boundary condition studied by Anum Tanveer et al. [20]. Recently, the influence of wall properties on the peristaltic flow of a nanofluid is discussed by Mustafa et al. [21].

Flow analysis of non-Newtonian fluids has growing interest in last decades. These type of fluid occur in engineering and biology. Some common examples of non-Newtonian fluids are paint, blood (at low shear rates), honey, condensed milk, shampoo etc. Due to their existence in biological and in industry, research on non-Newtonian fluids has been presented through different flow geometry. The mathematical formulation of non-Newtonian fluids in general is complex. Frequently used non-Newtonian fluids are Jeffrey fluid, Williamson, Maxwell, Power law fluid etc. Eyring-Powell fluid has certain advantage over other non-Newtonian fluid. The main advantage of Eyring-Powell fluid model is to recover the accurate results of Newtonian fluid behaviour at low and high shear rates. Powell and Eyring was first to proposed a model in 1944 known as Eyring-Powell fluid model [22]. The literature on peristaltic flow of Eyring-Powell fluid has grown during the last few years (see ref [23]-[27]) but information regarding the peristaltic flow of Eyring-Powell nanofluid is yet limited. Best of author knowledge, recently in 2017 Anum Tanveer et al. [28] studied the mixed convection peristaltic flow using Eyring-Powell nanofluid model in a channel with compliant walls.

The objective of present paper is to explore the effect of MHD on the peristaltic transport of Eyring-Powell nanofluid in a non uniform channel with the consideration of boundary conditions. The paper is organized in the following fashion. In section 1, the mathematical formulation of the problem have been constructed by employing the wave frame and then reduced by assumptions of long wavelength and low Reynolds number approximation. In section 2, series solution for velocity, concentration and temperature have been obtained by using Homotopy Analysis Method (HAM) [29-30]. In the last section, behaviors of Brownian motion parameter (Nb), thermophoresis parameter (Nt) on the non-uniform channel are shown graphically.

2. Mathematical Formulation

Let us consider the peristaltic Transport of Eyring-Powell nanofluid through a two dimensional non-uniform channel with the sinusoidal wave propagating towards down its walls. The nanofluid is electrically conducting by an external magnetic field B_0. Here we consider the Cartesian coordinate system $(\tilde{X}, \tilde{Y})$ such that $\tilde{X}$-axis is considered along the center line in the direction of wave propagation and $\tilde{Y}$-axis is transverse. The equation of the wall surface can be written as

$$\tilde{h}\left(\tilde{X}, \tilde{t}\right) = a(\tilde{X}) + b\sin\left[\frac{2\pi}{\lambda}\left(\tilde{X} - c\tilde{t}\right)\right]. \tag{2.1}$$

Here $a(\tilde{X}) = a_{20} + k\tilde{X}$ is the channel half width, λ is the wavelength, $\tilde{t}$ is the time and b represents the wave amplitude. Let $\tilde{U}$ and $\tilde{V}$ be the velocity components along the $\tilde{X}$ and $\tilde{Y}$ directions, respectively, in the fixed frame. The velocity V is given by

$$V = \left[\tilde{U}\left(\tilde{X}, \tilde{Y}, \tilde{t}\right), \tilde{V}\left(\tilde{X}, \tilde{Y}, \tilde{t}\right), 0\right]. \tag{2.2}$$

The shear of non-Newtonian fluid is considered to the study of Eyring-Powell fluid model. The stress tensor of Eyring-Powell fluid model is [31]

$$\tilde{S} = \mu\nabla\tilde{V} + \frac{1}{\beta}\sinh^{-1}\left(\frac{1}{c^*}\nabla\tilde{V}\right), \tag{2.3}$$

where μ is the viscosity, β and c^* are the material constants of Eyring-Powell fluid. Thus, equations embodying the conservation principles of mass, momentum, energy and nanoparticle mass transfer for the governing flow problem of an Eyring-Powell nanofluid can be written as

The continuity equation:

$$\frac{\partial\tilde{U}}{\partial\tilde{X}} + \frac{\partial\tilde{U}}{\partial\tilde{Y}} = 0. \tag{2.4}$$

The momentum equation:

(2.5)
$$\rho_f\left(\frac{\partial\tilde{U}}{\partial\tilde{t}}+\tilde{U}\frac{\partial\tilde{U}}{\partial\tilde{X}}+\tilde{V}\frac{\partial\tilde{U}}{\partial\tilde{Y}}\right)=-\frac{\partial\tilde{p}}{\partial\tilde{X}}+\left(\mu+\frac{1}{\beta c^*}\right)\left(\frac{\partial^2\tilde{U}}{\partial\tilde{X}^2}+\frac{\partial^2\tilde{U}}{\partial\tilde{Y}^2}\right)-\sigma B_0^2\tilde{U}$$
$$-\frac{1}{2\beta c^{*3}}\left\{\left(\frac{\partial\tilde{U}}{\partial\tilde{X}}\right)^2+\left(\frac{\partial\tilde{U}}{\partial\tilde{Y}}\right)^2+2\left(\frac{\partial\tilde{U}}{\partial\tilde{X}}\right)\left(\frac{\partial\tilde{U}}{\partial\tilde{Y}}\right)\right\}$$
$$\left(\frac{\partial^2\tilde{U}}{\partial\tilde{X}^2}+\frac{\partial^2\tilde{U}}{\partial\tilde{Y}^2}\right)+\rho_f g\kappa\left(\tilde{T}-\tilde{T}_0\right)+\rho_f g\kappa\left(\tilde{C}-\tilde{C}_0\right),$$

(2.6)
$$\rho_f\left(\frac{\partial\tilde{V}}{\partial\tilde{t}}+\tilde{U}\frac{\partial\tilde{V}}{\partial\tilde{X}}+\tilde{V}\frac{\partial\tilde{V}}{\partial\tilde{Y}}\right)=-\frac{\partial\tilde{p}}{\partial\tilde{Y}}+\left(\mu+\frac{1}{\beta c^*}\right)\left(\frac{\partial^2\tilde{V}}{\partial\tilde{X}^2}+\frac{\partial^2\tilde{V}}{\partial\tilde{Y}^2}\right)-\sigma B_0^2\tilde{V}$$
$$-\frac{1}{2\beta c^{*3}}\left\{\left(\frac{\partial\tilde{V}}{\partial\tilde{X}}\right)^2+\left(\frac{\partial\tilde{V}}{\partial\tilde{Y}}\right)^2+2\left(\frac{\partial\tilde{V}}{\partial\tilde{X}}\right)\left(\frac{\partial\tilde{V}}{\partial\tilde{Y}}\right)\right\}\left(\frac{\partial^2\tilde{V}}{\partial\tilde{X}^2}+\frac{\partial^2\tilde{V}}{\partial\tilde{Y}^2}\right).$$

The energy equation

$$\begin{aligned}(\rho c)_f\left(\frac{\partial\tilde{T}}{\partial\tilde{t}}+\tilde{U}\frac{\partial\tilde{T}}{\partial\tilde{X}}+\tilde{V}\frac{\partial\tilde{T}}{\partial\tilde{Y}}\right) &= k^*\left(\frac{\partial^2\tilde{T}}{\partial\tilde{X}^2}+\frac{\partial^2\tilde{T}}{\partial\tilde{Y}^2}\right)+(\rho c)_p D_B\left(\frac{\partial\tilde{C}}{\partial\tilde{X}}+\frac{\partial\tilde{C}}{\partial\tilde{Y}}\right)\left(\frac{\partial\tilde{T}}{\partial\tilde{X}}+\frac{\partial\tilde{T}}{\partial\tilde{Y}}\right)\\ &\quad +(\rho c)_p\frac{D_T}{T_m}\left(\frac{\partial^2\tilde{T}}{\partial\tilde{X}^2}+\frac{\partial^2\tilde{T}}{\partial\tilde{Y}^2}\right)^2.\end{aligned}\tag{2.7}$$

The concentration equation

$$\frac{\partial\tilde{C}}{\partial\tilde{t}}+\tilde{U}\frac{\partial\tilde{C}}{\partial\tilde{X}}+\tilde{V}\frac{\partial\tilde{C}}{\partial\tilde{Y}}=D_B\left(\frac{\partial^2\tilde{C}}{\partial\tilde{X}^2}+\frac{\partial^2\tilde{C}}{\partial\tilde{Y}^2}\right)+\frac{D_T}{T_m}\left(\frac{\partial^2\tilde{T}}{\partial\tilde{X}^2}+\frac{\partial^2\tilde{T}}{\partial\tilde{Y}^2}\right).\tag{2.8}$$

Here $\tilde{p}$ is the pressure, ρ_f is the density of the fluid, σ is the electrical conductivity of the fluid, B_0 is the applied magnetic field, g is the acceleration due to gravity, κ is the volume expansion coefficient, $\tilde{T}$ is the temperature of the fluid, $\tilde{C}$ is the nanoparticle concentration, $(\rho c)_f$ is the heat capacity of the fluid, k^* is the thermal conductivity, $(\rho c)_p$ is the effective heat capacity of the nanoparticle material, D_B is the Brownian diffusion coefficient, D_T is thermophoresis diffusion and T_m is the fluid mean temperature. The relations between the laboratory and wave frame are introduced through

$$\begin{aligned}&\tilde{x}=\tilde{X}-c\tilde{t}, && \tilde{y}=\tilde{Y},\\ &\tilde{u}(\tilde{x},\tilde{y})=\tilde{U}-c, && \tilde{v}(\tilde{x},\tilde{y})=\tilde{V},\end{aligned}\tag{2.9}$$

where $(\tilde{u}, \tilde{v})$ and $(\tilde{x}, \tilde{y})$ indicate the velocity components and coordinates in the wave frame.

The corresponding boundary conditions for the above problem is given by

$$\left.\begin{array}{ll} \tilde{\psi} = 0\ , \tilde{u} = \frac{\partial \tilde{\psi}}{\partial \tilde{y}} = 0\ ,\ \tilde{T} = \tilde{T}_0,\ \tilde{C} = \tilde{C}_0 & at \quad \tilde{y} = 0 \\ \tilde{\psi} = q,\ \tilde{u} = \frac{\partial \tilde{\psi}}{\partial \tilde{y}} = -c,\ \tilde{T} = \tilde{T}_1,\ \tilde{C} = \tilde{C}_1 & at \quad \tilde{y} = \tilde{h} = a(\tilde{x}) + b\sin\frac{2\pi}{\lambda}(\tilde{x}) \end{array}\right\}. \tag{2.10}$$

We introduce the following non-dimensional quantities

$$\left.\begin{array}{l} \psi = \frac{\tilde{\psi}}{ca},\ B = \frac{1}{\mu\beta c^*},\ A = \frac{Bc^2}{2a^2c^{*2}},\ X = \frac{\tilde{X}}{\lambda},\ x = \frac{\tilde{x}}{\lambda},\ Y = \frac{\tilde{Y}}{a},\ y = \frac{\tilde{y}}{a}, \\ t = \frac{c\tilde{t}}{\lambda},\ p = \frac{a^2\tilde{p}}{c\lambda\mu}v = \frac{\tilde{v}}{c},\ \delta = \frac{a}{\lambda},\ u = \frac{\tilde{u}}{c},\ Re = \frac{2\rho_f ca}{\mu},\ M = \sqrt{\frac{\sigma}{\mu}}B_0 a, \\ \beta^* = \frac{k^*}{(\rho c)_f}, \mathrm{Pr} = \frac{\nu}{\beta_*}, F = \frac{q}{ca},\ Gr = \frac{\rho_f g k a^2\left(\tilde{T}_1 - \tilde{T}_0\right)}{c\mu},\ Br = \frac{\rho_f g k a^2\left(\tilde{C}_1 - \tilde{C}_0\right)}{c\mu}, \\ Nb = \frac{(\rho c)_p D_B\left(\tilde{C}_1 - \tilde{C}_0\right)}{(\rho c)_f \nu},\ \alpha = \frac{b}{a_{20}}\ ,\ Nt = \frac{(\rho c)_p D_T\left(\tilde{T}_1 - \tilde{T}_0\right)}{(\rho c)_f T_m \nu}, \\ \Omega = \frac{\tilde{C} - \tilde{C}_0}{\tilde{C}_1 - \tilde{C}_0},\ \theta = \frac{\tilde{T} - \tilde{T}_0}{\tilde{T}_1 - \tilde{T}_0},\ h = \frac{\tilde{h}}{a_{20}} = 1 + \frac{\lambda k x}{a_{20}} + \alpha\sin 2\pi x. \end{array}\right\} \tag{2.11}$$

The non-dimensional symbols of the above mentioned quantities are as follows: A and B are the non-dimensional Eyring-Powell fluid parameters, Pr is the prandtl number, Gr and Br are the Grashof numbers corresponding to the local temperature and local nanoparticles mass transfer respectively, Nb is the Brownian motion parameter, Nt is the thermophoresis parameter, the Hartmann number M, the temperature distribution θ, Ω is the mass concentration, p is the dimensionless pressure, ψ is the stream function, x is the non-dimensional axial coordinate, y is the non-dimensional transverse coordinate, (u,v) is the velocity components, F is the dimensionless average flux in the wave frame, ν is the nanofluid kinematic viscosity and α is the amplitude ratio.

The nonlinear terms in the momentum equation are determined to be zero $(Re\delta^2)$, where $Re = \frac{2\rho_f ca}{\mu}$ is the Reynolds number and $\delta = \frac{a}{\lambda}$ is the wave number and using non-dimensional quantities. Introducing the velocity fields in terms of stream

functions $\left(u = \frac{\partial \psi}{\partial y}, v = -\delta \frac{\partial \psi}{\partial x}\right)$ with long wavelength and low Reynolds number approximation, the basic equations (2.1)-(2.11) reduce to

$$\frac{\partial p}{\partial x} = (1+B)\frac{\partial^3 \psi}{\partial y^3} - A\left(\frac{\partial^2 \psi}{\partial y^2}\right)^2 \frac{\partial^3 \psi}{\partial y^3} - M^2 \frac{\partial \psi}{\partial y} + Gr\theta + Br\Omega, \tag{2.12}$$

$$\frac{\partial p}{\partial y} = 0, \tag{2.13}$$

$$\frac{\partial^2 \theta}{\partial y^2} + \Pr Nb \frac{\partial \theta}{\partial y}\frac{\partial \Omega}{\partial y} + \Pr Nt \left(\frac{\partial \theta}{\partial y}\right)^2 = 0, \tag{2.14}$$

$$\frac{\partial^2 \Omega}{\partial y^2} + \frac{Nt}{Nb}\frac{\partial^2 \theta}{\partial y^2} = 0. \tag{2.15}$$

The corresponding dimensionless boundary conditions can be written in the following form

$$\left.\begin{array}{lll} \psi = 0\ , \frac{\partial \psi}{\partial y} = 0,\ \theta = 0,\ \Omega = 0 & at & y = 0 \\ \psi = F,\ \frac{\partial \psi}{\partial y} = -1,\ \theta = 1,\ \Omega = 1 & at & y = h = 1 + \frac{\lambda k x}{a_{20}} + \alpha \sin 2\pi x \end{array}\right\}, \tag{2.16}$$

where the dimensionless time mean flow rate F is the wave frame is related to the dimensionless time mean flow rate Θ in the laboratory frame as follows

$$\Theta = F + 1, \qquad F = \int_0^h \frac{\partial \psi}{\partial y}\, dy. \tag{2.17}$$

Differentiating equation (2.12) with respect to 'y', by yields

$$(1+B)\frac{\partial^4 \psi}{\partial y^4} - A\frac{\partial}{\partial y}\left(\left(\frac{\partial^2 \psi}{\partial y^2}\right)^2 \frac{\partial^3 \psi}{\partial y^3}\right) - M^2 \frac{\partial^2 \psi}{\partial y^2} + Gr\frac{\partial \theta}{\partial y} + Br\frac{\partial \Omega}{\partial y} = 0. \tag{2.18}$$

3. Method of Solution

The solution of the present problem is obtained by using a powerful analytical techniques, namely the Homotopy Analysis Method (HAM). In the present case we seek initial guess to be [32].

$$\psi_0(y) = \frac{y\left(4Fh^3 - Fy^3 + h^4 - hy^3\right)}{3h^4}, \tag{3.1}$$

$$\theta_0(y) = \frac{y}{h}, \tag{3.2}$$

$$\Omega_0(y) = \frac{y}{h}. \tag{3.3}$$

The corresponding auxiliary linear operators are

$$L_\psi = \frac{\partial^5}{\partial y^5}, \qquad L_\theta = \frac{\partial^2}{\partial y^2}, \qquad L_\Omega = \frac{\partial^2}{\partial y^2} \tag{3.4}$$

with property

$$L_\psi\left[C_1 + C_2 y + C_3\frac{y^2}{2} + C_4\frac{y^3}{6} + C_5\frac{y^4}{24}\right] = 0, \qquad L_\theta\left[C_1 + C_2 y\right] = 0, \qquad L_\Omega\left[C_1 + C_2 y\right] = 0, \tag{3.5}$$

where C_1, C_2, C_3, C_4 and C_5 are integral constants.

Now we define the non linear operators as

$$N\left[\phi_\psi(y;q)\right] = -2A\frac{\partial^5\psi}{\partial y^5} - A\left(\left(\frac{\partial^2\psi}{\partial y^2}\right)^2\frac{\partial^3\psi}{\partial y^3}\right) + (1+B)\frac{\partial^5\psi}{\partial y^5} - M^2\frac{\partial^2\psi}{\partial y^2} + Gr\frac{\partial\theta}{\partial y} + Br\frac{\partial\Omega}{\partial y}, \tag{3.6}$$

$$N\left[\phi_\theta(y;q)\right] = \frac{\partial^2\theta}{\partial y^2} + \Pr Nb\frac{\partial\theta}{\partial y}\frac{\partial\Omega}{\partial y} + \Pr Nt\left(\frac{\partial\theta}{\partial y}\right)^2, \tag{3.7}$$

$$N\left[\phi_\Omega(y;q)\right] = \frac{\partial^2\Omega}{\partial y^2} + \frac{Nt}{Nb}\frac{\partial^2\theta}{\partial y^2}. \tag{3.8}$$

Using the above definition, we construct the zeorth-order deformation equations by

$$(1-q)\,L\left[\phi_\psi(y;q) - \psi_0(y)\right] = qH_\psi h_\psi N_\psi\left[\phi_\psi(y;q)\right], \tag{3.9}$$

$$(1-q)\,L\left[\phi_\theta\left(y;q\right)-\theta_0\left(y\right)\right]=qH_\theta h_\theta N_\theta\left[\phi_\theta\left(y;q\right)\right], \tag{3.10}$$

$$(1-q)\,L\left[\phi_\Omega\left(y;q\right)-\Omega_0\left(y\right)\right]=qH_\Omega h_\Omega N_\Omega\left[\phi_\Omega\left(y;q\right)\right], \tag{3.11}$$

where $q\in[0,1]$ is the embedding parameter, h_ψ, h_θ, h_Ω are the auxiliary parameters, L is an auxiliary linear operator. It is obvious that when embedding parameter $q=0$ and $q=1$ equations (3.9)-(3.11) becomes

$$\left.\begin{array}{l}\phi_\psi(y;0)=\psi_0(y),\phi_\theta(y;0)=\theta_0(y),\phi_\Omega(y;0)=\Omega_0(y)\\ \phi_\psi(y;1)=\psi(y),\phi_\theta(y;1)=\theta(y),\phi_\Omega(y;1)=\Omega(y)\end{array}\right\}. \tag{3.12}$$

From (3.9)-(3.12) equation we can easily found the system of equations with their relevant boundary conditions. According to the methodology of homotopy analysis method the solutions are given by

$$\theta\left(y;q\right)=\theta_0(y)+h_\theta\theta_1(y)+h_\theta^2\theta_2(y)+... \tag{3.13}$$

$$\Omega\left(y;q\right)=\Omega_0(y)+h_\Omega\Omega_1(y)+h_\Omega^2\Omega_2(y)+... \tag{3.14}$$

$$\psi\left(y;q\right)=\psi_0(y)+h_\psi\psi_1(y)+h_\psi^2\psi_2(y)+... \tag{3.15}$$

The solutions for temperature, concentration and velocity ($u=\frac{\partial\psi}{\partial y}$) are evaluated using equations (3.13)-(3.15) and they can be written as

(3.16)

$$\begin{aligned}\theta\left(y;q\right)=\ &\tfrac{y}{h}+2h_\theta\left(Nb+Nt\right)\left(\tfrac{\mathrm{Pr}}{h^2}\right)\tfrac{y^2}{2!}+h_\theta^2\left(Nb+Nt\right)\left(\tfrac{\mathrm{Pr}}{h^2}\right)\tfrac{y^2}{2!}+h_\theta^2h_\Omega\left(Nb+Nt\right)^2\left(\tfrac{\mathrm{Pr}^2}{h^3}\right)\tfrac{y^3}{3!}\\ &+2h_\theta^3Nt\left(Nb+Nt\right)^2\left(\tfrac{\mathrm{Pr}^3}{h^4}\right)\tfrac{y^4}{4!},\end{aligned}$$

(3.17)

$$\Omega\left(y;q\right)=\tfrac{y}{h}+2h_\Omega\left(1+\tfrac{Nt}{Nb}\right)\tfrac{y}{h}+h_\Omega^2\left(1+\tfrac{Nt}{Nb}\right)\tfrac{y}{h}+h_\Omega h_\theta Nt\left(1+\tfrac{Nt}{Nb}\right)\left(\tfrac{\mathrm{Pr}}{h^2}\right)\tfrac{y^2}{2!},$$

(3.18)

$$
\begin{aligned}
&u\left(y;q\right)=\\
&\tfrac{1}{3}+\tfrac{4F}{3h}-\left(\tfrac{8}{h^3}+\tfrac{8F}{h^4}\right)\tfrac{y^3}{3!}-32h_\psi A\left(\tfrac{1}{h^3}+\tfrac{F}{h^4}\right)\tfrac{y^3}{3!}+2h_\psi a_0\tfrac{y^4}{4!}+2h_\psi A\left(\tfrac{5225472}{1591}\right)\left(\tfrac{1}{h^3}+\tfrac{F}{h^4}\right)^3\\
&\tfrac{y^8}{8!}-32h_\psi^2\left(\tfrac{1}{h^3}+\tfrac{F}{h^4}\right)\tfrac{y^3}{3!}\tfrac{y^4}{4!}+2A\,h_\psi^2a_0+2h_\psi^2A\left(\tfrac{5225472}{1591}\right)\left(\tfrac{1}{h^3}+\tfrac{F}{h^4}\right)^2\tfrac{y^8}{8!}\\
&-16A(1+B)\,h_\psi^2\left(\tfrac{1}{h^3}+\tfrac{F}{h^4}\right)\tfrac{y^4}{4!}+(1+B)h_\psi^2a_0\,\tfrac{y^5}{5!}(1+B)h_\psi^2A\left(\tfrac{5225472}{1591}\right)\left(\tfrac{1}{h^3}+\tfrac{F}{h^4}\right)^2\tfrac{y^9}{9!}\\
&+16M^2h_\psi^2A\left(\tfrac{1}{h^3}+\tfrac{F}{h^4}\right)\tfrac{y^6}{6!}-M^2h_\psi^2a_0\,\tfrac{y^7}{7!}-M^2h_\psi^2A\left(\tfrac{5225472}{1591}\right)\left(\tfrac{1}{h^3}+\tfrac{F}{h^4}\right)^2\tfrac{y^{11}}{11!}\\
&+h_\psi h_\theta Gr\tfrac{\mathrm{Pr}}{h^2}\left(Nb+Nt\right)\tfrac{y^5}{5!}+h_\Omega h_\theta Br\tfrac{\mathrm{Pr}}{h^2}\left(1+\tfrac{Nt}{Nb}\right)\tfrac{y^5}{5!},
\end{aligned}
$$

where $a_0=\left(8(1+B)\left(\tfrac{1}{h^3}+\tfrac{F}{h^4}\right)+8M^2\left(\tfrac{1}{h^3}+\tfrac{F}{h^4}\right)+\tfrac{Gr}{h}+\tfrac{Br}{h}\right)$.

4. Results and Discussion

This section prepared to describe the results of our problem graphically using Mathematica program. It consists of three parts; the first part illustrates the impact of some physical parameters on the velocity distribution. However in the second part the evaluation of temperature distribution with different parameters discussed and the third part illustrates the concentration with different parameters.

4.1. Velocity profile

Figures 1 to 8, are plotted to show the behavior of different parameters on the velocity distribution u. Fig. 1 shows that the velocity decreases with an increase in the Eyring-Powell fluid parameter A, which appears with the non-linear term of the governing momentum. Fig. 2 includes the effect of Eyring-Powell fluid parameter B. The velocity appears to increase when B is increased. Fig. 3 captures the effects of Hartman number M on the velocity. Here it is observe that velocity is a decreasing function of M. Fig. 4 shows that as Grashof number Gr increases the velocity profile increases. Fig. 5 includes the effect of local nanoparticle Grashof number Br. Here velocity appears to decreases when Br is increased. In Fig. 6, the effect of Brownian motion parameter Nb on velocity is plotted. The velocity appears to increases when Brownian motion parameter Nb increased. The Fig. 7 is the effect thermophoresis

parameter Nt. The velocity appears to decreases when thermophoresis parameter Nt increased. Fig. 8, shows the effect of Prandtl number Pr. The velocity appears to increases when Prandtl number Pr increased.

4.2. Temperature profile

Figures 9 to 11, are plotted to show the behavior of different parameters on the temperature distribution θ. Fig. 9 shows that the temperature increases with an increase in the Brownian motion parameter Nb. Fig. 10 captures the effect of thermophoresis parameter Nt on the temperature. It shows that the temperature decreases when the thermophoresis parameter increases. Fig. 11 includes the effect of Prandtl number Pr on the temperature, It is clear that the temperature decreases when the Prandtl number Pr increased.

4.3. Concentration profile

Figures 12 to 14 describe the variation of the concentration profile for several values of the Prandtl number Pr, thermophoresis parameter Nt and the Brownian motion parameter Nb. In Fig. 12 we observe that the concentration profile increases with an increase in Nb. Fig. 13 captures the effect of thermophoresis parameter Nt on the concentration profile. We can notice that the concentration decreases when the thermophoresis parameter increases. Fig. 14 includes the effect of prandtl number Pr on the concentration. Here the concentration increases when the Prandtl number Pr increases.

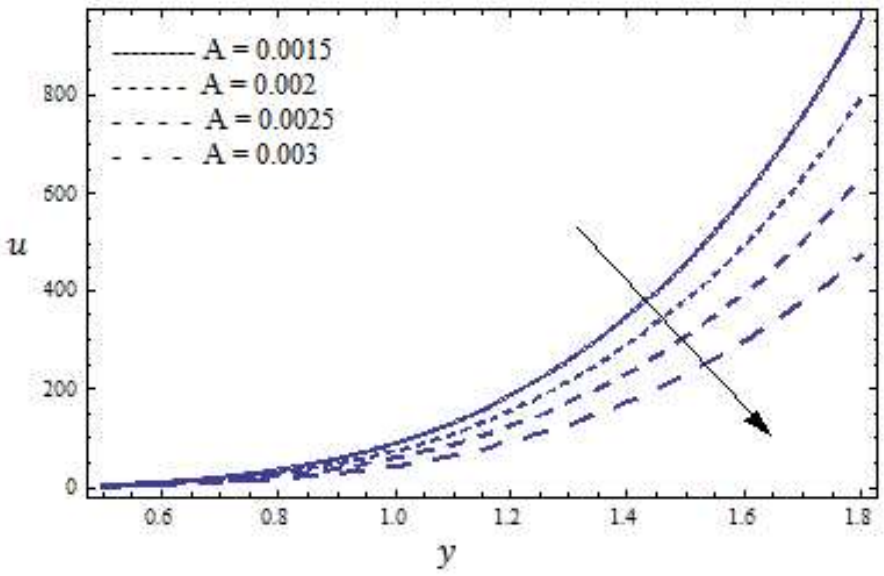

Fig. 1 Velocity profile for different values of A for fixed B=2.0, M=1.2, Gr=0.4, Br=0.3, Pr=7.0, Nt=0.3, Nb=0.2, x=0.1, θ=0.15.

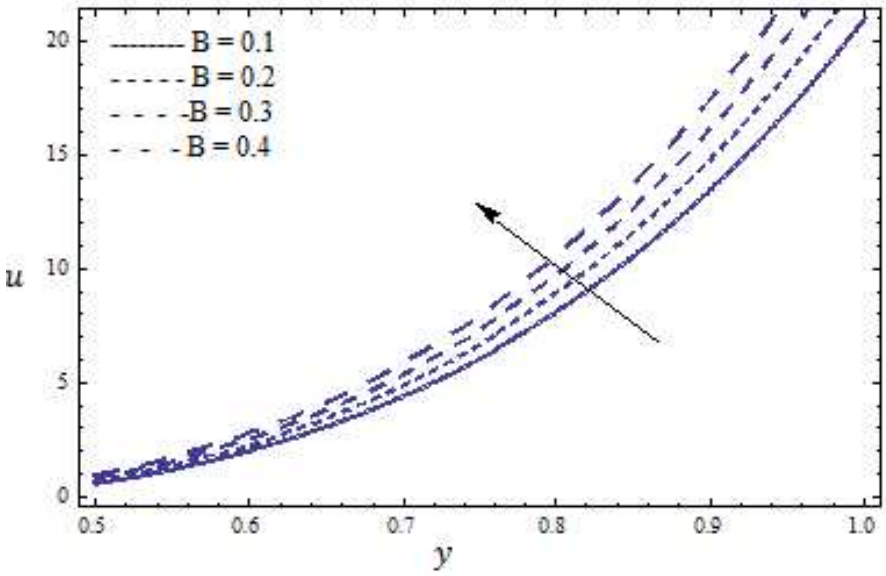

Fig. 2 Velocity profile for different values of B for fixed A=0.002, M=1.2, Gr=0.4, Br=0.3, Pr=7.0, Nt=0.3, Nb=0.2, x=0.1, θ=0.15.

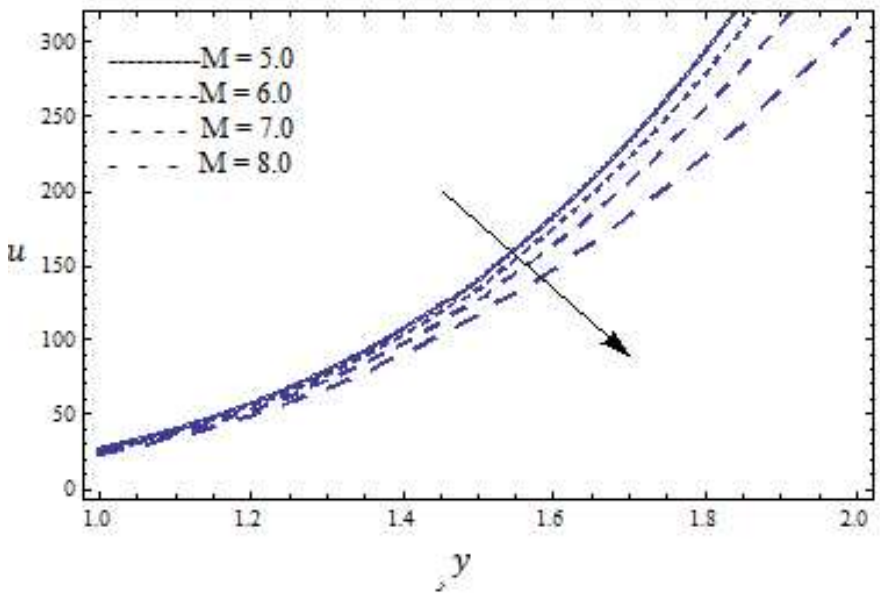

Fig. 3 Velocity profile for different values of M for fixed A=0.001, B=2.0, Gr=0.4, Br=0.3, Pr=7.0 , Nt=0.3, Nb=0.2, x=0.1, θ=0.15.

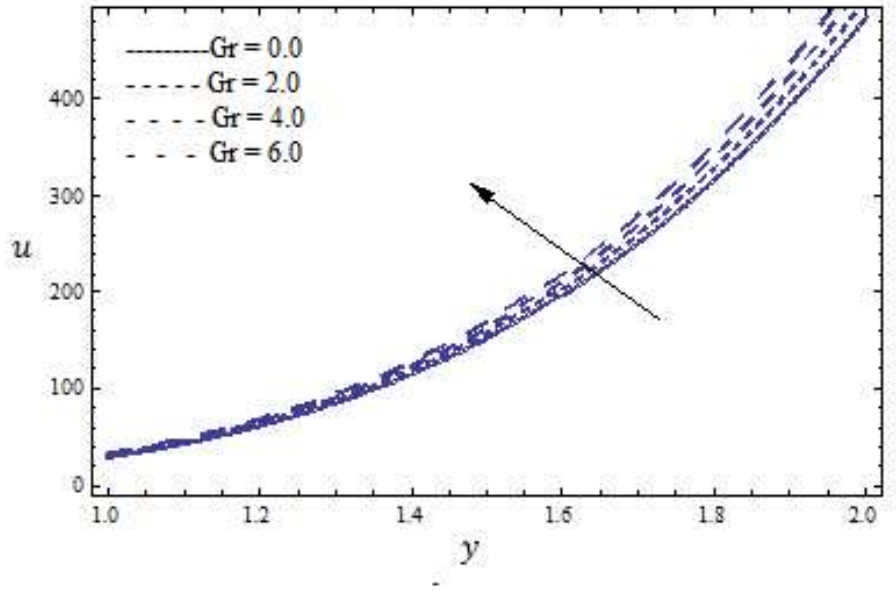

Fig. 4 Velocity profile for different values of Gr for fixed A=0.002, B=0.5, M=0.5, Br=6.0, Pr=7.0, Nt=0.7, Nb=0.6, x=0.1, θ=0.15.

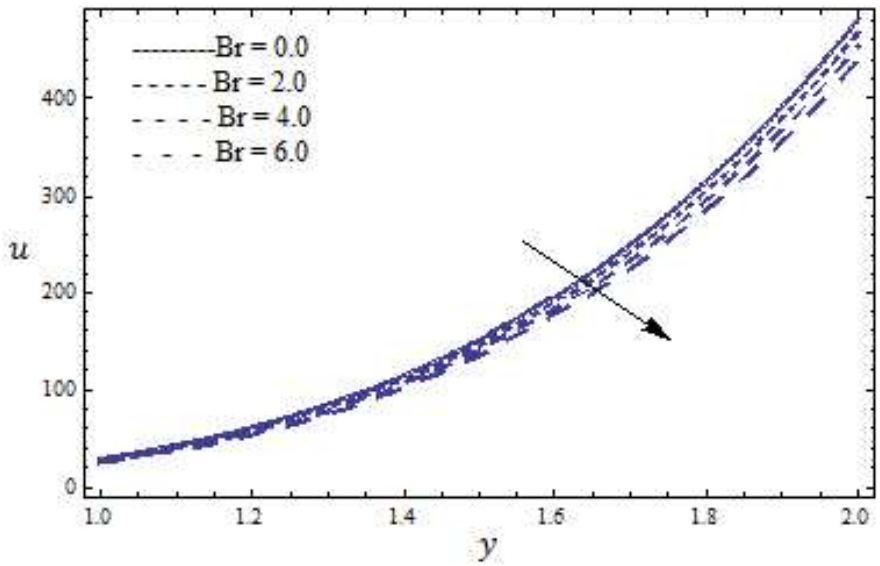

Fig. 5 Velocity profile for different values of Br for fixed A=0.002, B=0.5, M=0.5, Gr=6.0, Pr=7.0, Nt=0.7, Nb=0.6, x=0.1, θ=0.15.

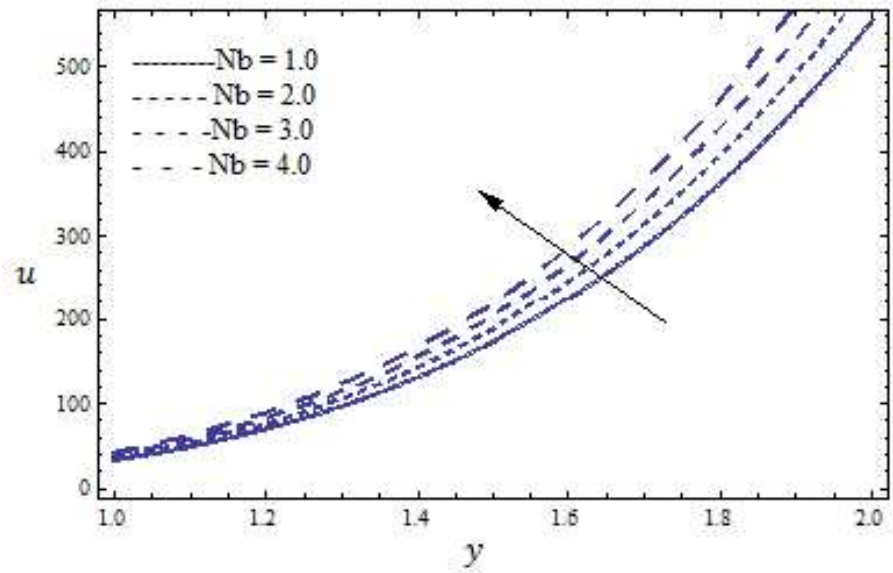

Fig. 6 Velocity profile for different values of Nb for fixed A=0.002, B=0.5, M=0.5, Gr=2.0, Br=6.0, Pr=7.0, Nt=4.0, x=0.1, θ=0.15.

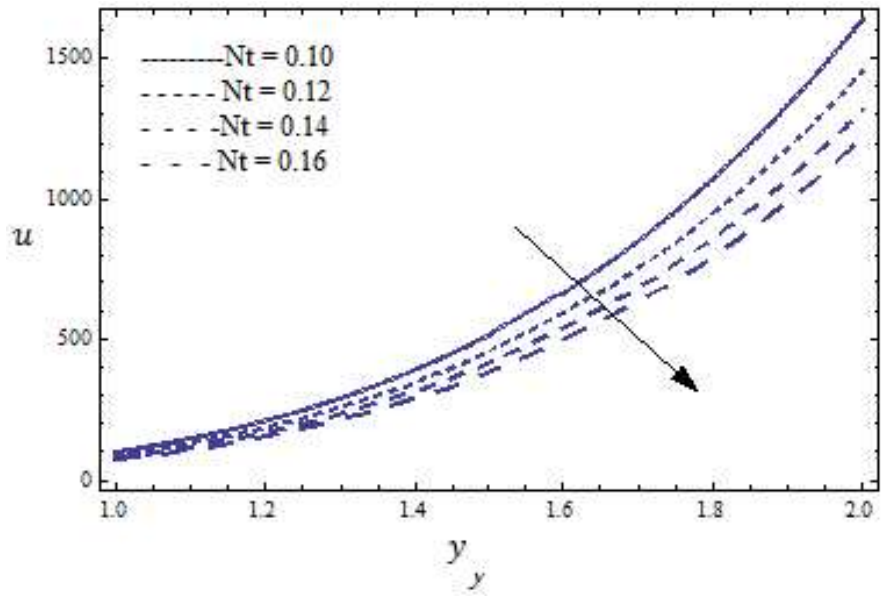

Fig.7 Velocity profile for different values of Nt for fixed A=0.002, B=0.5, M=0.5, Gr=2.0, Br=6.0, Pr=7.0, Nb=0.6, x=0.1, θ=0.15.

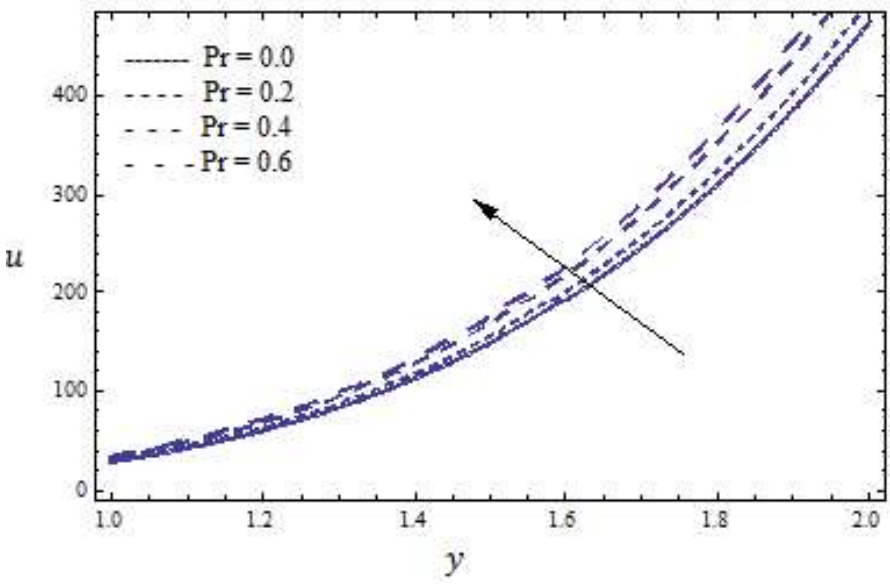

Fig. 8 Velocity profile for different values of Pr for fixed A=0.002, B=0.5, M=0.5, Gr=2.0, Br=6.0, Nb=0.2, Nt=4.0, x=0.1, θ=0.15.

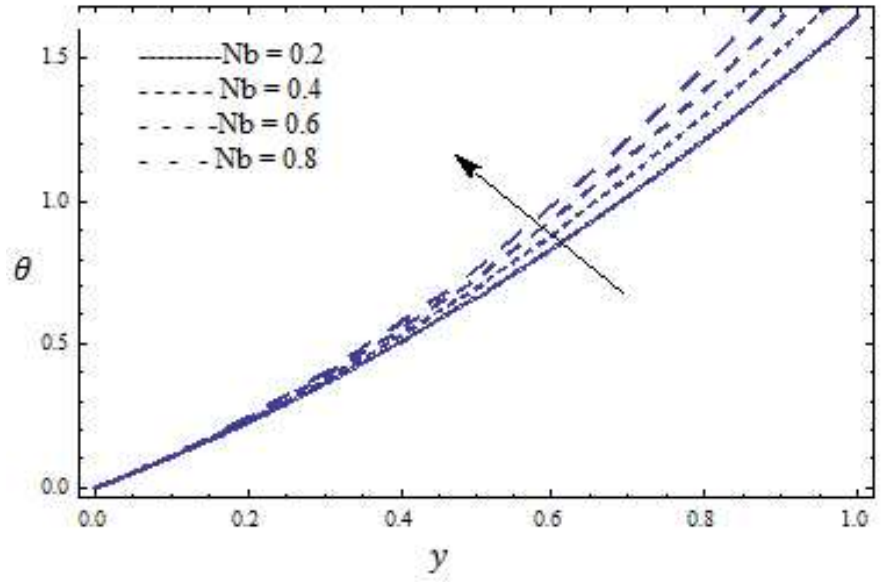

Fig. 9 Temperature profile for different values of Nb for fixed Pr=7.0, Nt=0.7 , x=0.2, θ=0.15.

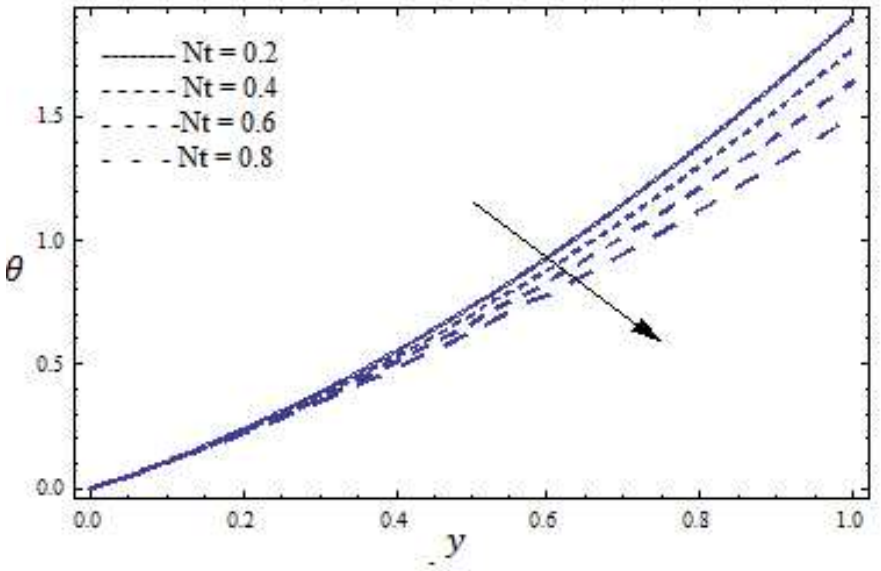

Fig. 10 Temperature profile for different values of Nt for fixed Pr=7.0, Nb=0.5, x=0.2, θ=0.15.

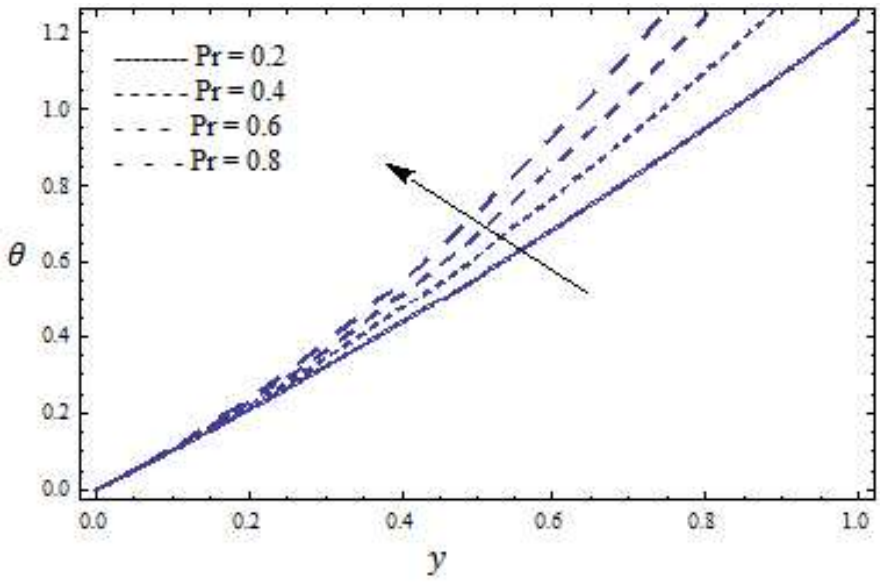

Fig. 11 Temperature profile for different values of Pr for fixed Nt=0.3, Nb=0.5, x=0.2, θ=0.15.

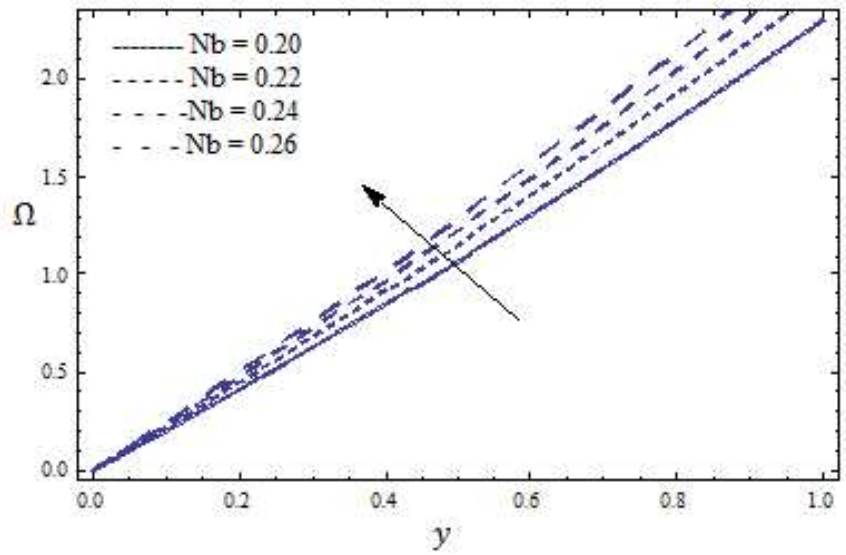

Fig .12 Concentration profile for different values of Nb for fixed Nt=0.4,Pr=7.0, x=0.2, θ=0.15.

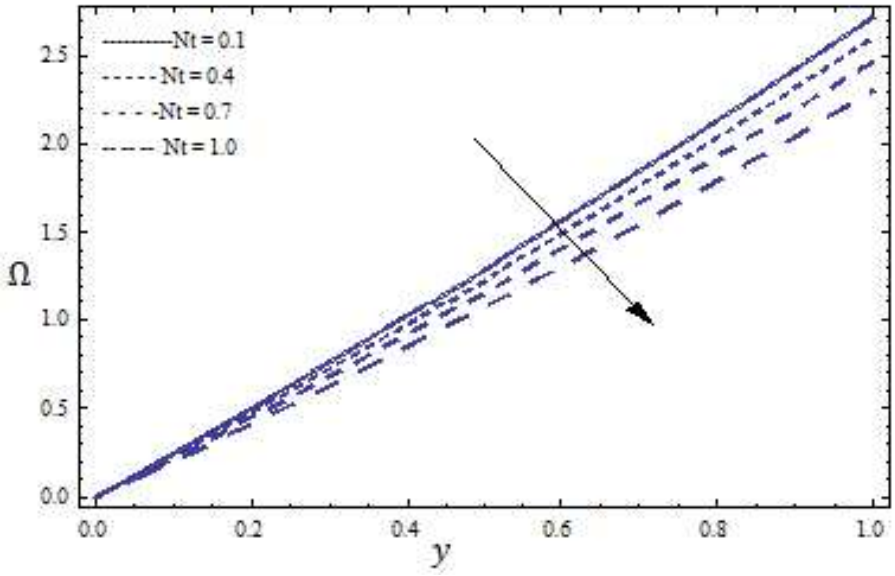

Fig .13 Concentration profile for different values of Nt for fixed Nb=4.0, Pr=7.0, x=0.2, θ=0.15.

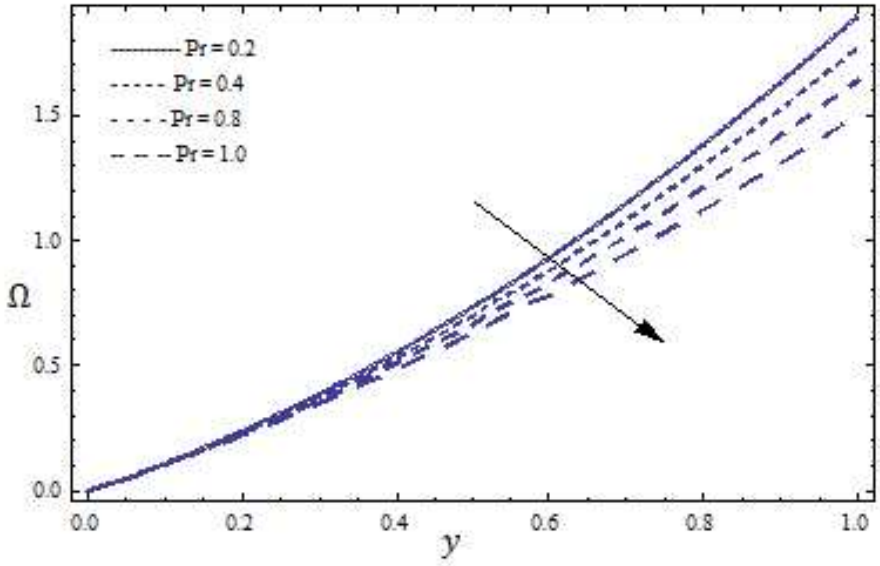

Fig. 14 Concentration profile for different values of Pr for fixed Nt=0.3, Nb=0.5, x=0.2, θ=0.15.

5. Concluding remarks

Peristaltic Transport of Eyring-Powell nanofluid in a non uniform channel is modelled in the presence of MHD. The main observations of the present analysis are as follows:

- The velocity profile gives opposite results with increasing values of Eyring-Powell fluid parameters A and B.
- It is observed that the magnetic parameter M and the Prandtl number Pr have opposite effects on the velocity.
- Dissimilar response of thermal Grashof number Gr and local nanoparticle Grashof number Br are noticed towards velocity of nanofluids.
- Similar behavior of velocity, temperature and concentration profiles is observed increases with an increase in Brownian motion parameter Nb and decreases with an increase in the thermophoresis parameter Nt.
- The temperature profile increases with an increase in the Prandtl number Pr and the concentration profile decreases with an increase in the Prandtl number Pr.

Acknowledgement

We would like to thank the editor and the referees for their constructive comments that significantly improved this manuscript. Author Asha S. K acknowledge the kind support of the University Grants Commission (UGC)(F510/3/DRS-III/2016(SAP-I)) Dated:29-Feb-2016. further, the author Sunitha G is thankful to University Grant Commission (UGC), New Delhi, for their financial support under National Fellowship for Higher Education of ST Students to persue M.Phil/Ph.D degree (201718-NFST-KAR-01215) Dated:01-April-2017.

References

[1] T. W. Latham, *Fluid motion in a peristaltic pump*, MS. Thesis, M. I. T, Cambridge, 1966.

[2] A. H. Shapiro and M. Y. Jaffrin, *Peristaltic Pumping*, Annual Review of Fluids Mechanics, **3** (1971), 13-16.

[3] K. S. Mekheimer, *Peristaltic flow of blood under effect of a magnetic field in a non-uniform channel*, Applied Mathematics and Computation, **153** (2004), 763-777.

[4] S. K. Asha and V. P. Rathod, *Effect of magnetic field and an endoscope on peristaltic motion*, Advance in applied Science Research, **4** (2012), 102-109.

[5] S. K. Asha and V. P. Rathod, *Peristaltic Transport of magnetic fluid in Uniform and Non-Uniform Annulus*, International journal of Mathematics Archive, **12** (2012), 1-11.

[6] S. K. Asha, *Peristaltic Transport of a magnetic fluid through porous media in a Uniform and Non-Uniform Annulus*, Journal of Global Research in Mathematical Archives, **6** (2014), 44-54.

[7] S. K. Asha and G. Sunita, *Effect of Couple Stress in Peristaltic Transport of Blood Flow by Homotopy Analysis Method*, Asian Journal of Science and Technology, **12** (2017), 6958-6964.

[8] M. Suryanarayana reddy, *study of MHD effects on peristaltic transport of non-newtonian fluid flows in channels and tubes*, JNTUA, 2010.

[9] T. Hayat, F.M. Abbasi, B. Ahamad and A. Alsaedi, *MHD Mixed convection peristaltic flow with variable viscosity and thermal conductivity*, Sains Malaysiana , **43** (2014), 1583-1590.

[10] Aaiza Gul, Ilyas khan, Sharidan Shafia, Asma Khalid and Arshad Khan, *Heat transfer in MHD mixed convection flow of a ferrofluid along a vertical channel*, PLOS ONE , **10** (2015), 1-14.

[11] F. M. Abbasi, T. Hayat and A. Alsaedi, *Numerical analysis for peristaltic motion of MHD Eyring-Prandtl fluid in an inclined symmetric cannel with inclined Magnetic field*, Journal of Applied Fluid Mechanics, **9** (2016), 389-396.

[12] Nabil T. M Eldabe, Osama M. Abo-Seida and Adel. S. Abo-Seliem, *Peristaltic transport of magnetohydrodynamic carreau nanofluid with heat and mass transfer inside asymmetric channel*, American Journal of Computational Mathematics, (2017), 1-20.

[13] Rizwan Ul Haq, Zakia Hamouch, S. T. Hussain and Toufik Mukkaoui *MHD mixed convection flow along a vertically heated sheet*, International Journal of Hydrogen Energy , (2017), 1-8.

[14] Hayat Ali and Ahmed Abdulhadi, *Influence of magnetic field on peristaltic transport for Eyring-Powell Fluid in a Symmetric Channel during a porous medium*, Mathematical Theory and Modelling, **9** (2017), 9-22.

[15] SUS Choi, *Enhancing thermal conductivity of the fluids with nanoparticles*, ASME Fluids Eng Div, **231** (1995), 99-105.

[16] N. S. Akbar, S. Nadeem, T. Hayat and A. A. Hendi, *Peristaltic flow of a nanofluid with slip effect*, ASME Fluids Eng Div, **47** (2011), 1283-1294.

[17] N. S. Akbar and S. Nadeem, *Endoscopic effects on peristaltic flow of nanofluid*, Commun Theor. Phys., **56** (2011), 761-768.

[18] Hayat T, Aqsa Saleem, Anum Tanveer and Fuad Alsaadi, *Numerical study for MHD peristaltic flow of Williamson nanofluid in an endoscope with partial slipand wall properties*, International Journal of heat and mass transfer, **114** (2017), 1181-1187.

[19] Akbar N.S and sohail Nadeem , *Mixed convection MHD peristaltic flow of a Jaffrey nanofluid with Newtonian heating*, Z. Naturforschnung, **68**(A) (2013), 433-441.

[20] Anum Tanveer, T. Hayat and Alsaedi, *Peristaltic flow of MHD Jaffrey nanofluid in a curved channel with convective boundary condition: a numerical study*, Natural computing Application forum, **30** (2018), 437-446.

[21] M. Mustafa, S. Hina, T. Hayat and Alsaedi, *Influence of wall properties on the peristaltic flow of a nanofluid: Analytic and Numerical solutions*, International Journal of Heat and Mass Transfer, **55** (2012), 4871-4877.

[22] RE. Powell and H. Eyring, *Mechanism for the relaxation theory of viscosity*, Nature, **154** (1994), 427-428.

[23] F. M. Abbasi, A. Alsaedi and T. Hayat, *Peristaltic Transport of Eyring-Powell fluid in a curved channel*, J. Aerosp. Eng., 2014.

[24] S. Nooren and M. Qasim, *Peristaltic flow of MHD Eyring-Powell fluid in a channel*, Eur. Phys. J. Plus, **91** (2017).

[25] T. Hayat, S. Irfan Shah, B. Ahmad and M. Mustafa, *Effect of slip on peristaltic flow of Powell-Eyring fluid in a symmetric channel*, Applied Bionics and Biomechanics, **11** (2014), 69-79.

[26] T. Hayat, Anum Tanveer, Humaira Yasmin and A. Alsaedi, *Effects of convective conditions and chemical reaction on peristaltic flow of eyring-powell fluid*, Applied Bionics and Biomechanics, **11** (2014), 221-233.

[27] S. Hina, M. Mustafa, T. Hayat and A. Alsaedi, *Peristaltic flow of Powell-Eyring in curved channel with heat transfer: A useful application in biomedicine*, Computer Methods and Programs in Biomedicine, **135** (2016), 89-100.

[28] Anum Tanveer, T. Hayat, Fuad Alsaadi and A. Alsaedi, *Mixed convection peristaltic flow of Eyring-Powell nanofluid in a curved channel with compliant walls*, Computers in Biology and Medicine, **82** (2017), 71-79.

[29] Mourad S. Semary and Hany N. Hassan, *The Homotopy Analysis Method for Strongly Nonlinear Initial Boundary Value Problems*, International Journal of Modern Mathematical Sciences, **3** (2014), 154-172.

[30] V. G. Gupta and Sumit Gupta, *Application of Homotopy Analysis Method for Solving nonlineae cauchy problem*, Surveys in Mathematics and its Applications, **7** (2012), 105-116.

[31] T. Hayat, A.B. Naseema Aslama, M. Rafiq and Faud E Alsaadi *hall and joule heating effects on peristaltic flow of powell-eyring liquid in an inclined symmetric channel*, Results in Physics , **7** (2017), 518-528.

[32] D. Rostamy, F. Zabihi and K. Karimi, *The Application of Homotopy Analysis Method for Solving the Prey and Predator Problem*, Applied Mathematical Sciences , **5** (2011), 639-650.

(1) Department of Mathematics, Karnatak University, Dharwad-580003, Karnataka, India

E-mail address: as.kotnur2008@gmail.com

(2) Research Scholar, Department of Mathematics, Karnatak University, Dharwad-580003, Karnataka, India

E-mail address: sunithag643@gmail.com